

See discussions, stats, and author profiles for this publication at: <https://www.researchgate.net/publication/40022492>

Micron-Sized Structure in a Thin Glycerol Film Revealed by Fluorescent Probes

ARTICLE in THE JOURNAL OF PHYSICAL CHEMISTRY B · DECEMBER 2009

Impact Factor: 3.3 · DOI: 10.1021/jp9058388 · Source: PubMed

CITATIONS

10

READS

21

3 AUTHORS:



Tie Xia

Tsinghua University

19 PUBLICATIONS 241 CITATIONS

SEE PROFILE



Liantuan Xiao

Shanxi University

134 PUBLICATIONS 445 CITATIONS

SEE PROFILE



Michel Orrit

Leiden University

207 PUBLICATIONS 8,978 CITATIONS

SEE PROFILE

Micron-Sized Structure in a Thin Glycerol Film Revealed by Fluorescent Probes

Ted Xia, Liantuan Xiao,[†] and Michel Orrit*

Molecular Nano-Optics and Spins, Huygens Laboratory, Leiden University, Niels Bohrweg 2, 2333CA Leiden, The Netherlands

Received: June 22, 2009; Revised Manuscript Received: September 23, 2009

We report on micrometer-sized structures in supercooled glycerol observed by imaging fluorescent probes at the temperatures close to, but above, the glass transition temperature (190 K). Two distinct heterogeneous patterns of the fluorescence intensity were detected, depending on how fast the sample was cooled down. In a slowly cooled sample, we observed a Swiss cheese-like pattern in which many micrometer-sized dark spots were nucleated in a bright background. A quickly cooled sample resulted in a spinodal decomposition pattern where many bright island-like features on micrometer scale were dispersed in a dark matrix. Similar patterns were seen earlier in triphenyl phosphite, another molecular liquid, which shows solid-like behavior at temperatures above its glass transition. Once the heterogeneous patterns are formed in the glycerol, they can persist for days, unless the samples are heated above 260 K for more than 10 h. Such heterogeneous patterns are ascribed to differential dye distributions in the glycerol film, pointing to long-lived and micrometer-scale density fluctuations in supercooled glycerol. The observation of such heterogeneity may provide additional understanding on how supercooled glycerol behaves before it turns into a glass.

Introduction

Many liquids can be cooled below their melting points without being crystallized and remain liquid-like until their glass transition temperatures T_g are reached. Along this cooling down, their viscosities increase enormously. The structural mechanism, through which the dynamics of supercooled liquids are slowed down and finally arrested, has been a mystery for more than half a century.¹ It is widely accepted that rearranging many molecules locally in a cooperative manner (forming locally favored structures) plays a key role in dynamical heterogeneity and glass formation.²

Heterogeneity has been observed in many glass forming systems by both experiments and computer simulations.^{3–5} However, there is no consensus on the structural origin, time, and length scales of those inhomogeneities. Molecular-scale spectroscopic techniques such as NMR^{6,7} and dielectric relaxation^{8,9} invariably find the relaxation time of heterogeneity comparable with molecular reorientation times in supercooled liquids and the length scales of a few nanometers. However, optical experiments, notably light and X-ray scattering,^{10,11} polarized hole-burning,^{12,13} and single-molecule spectroscopy,^{14,15} reveal much slower relaxation and longer length scales.

Recent single-molecule rotational diffusion measurements in a thin glycerol film showed that different single probe molecules rotate at different rates in the supercooled regime and that the distribution of rotation rates broadens upon approaching the glass transition temperature (190 K).¹⁶ This is consistent with previous observations of dynamical heterogeneity in supercooled glycerol by various techniques.^{8,9,17–19} In addition, Zondervan et al. found surprisingly long-lived inhomogeneity at temperatures well above T_g . The time scale is on the order of hours, which is about 6 orders of magnitude longer than the typical time for a glycerol molecule to reorient. Such long-lived heterogeneity strongly

suggests that some nearly static structures already exist at temperatures above T_g and form a solid-like network percolating in the supercooled liquid. Indeed, later rheological measurements on glycerol confirmed the existence of a solid-like network at temperatures well above the glass transition temperature.²⁰

Fluorescence imaging has been widely used to study phase separation in polymer blends^{21–23} and membrane-like systems^{24–26} where fluorescent probes are either chemically attached to the molecules of interest or doped directly into materials under investigation. When the phase separation is initiated, for example, by a temperature change, this process can be monitored by following the evolution of the fluorescence pattern.²⁶ Here, we used fluorescent dyes to image thin glycerol films at temperatures close to, but above, T_g , and we found two distinct heterogeneous dye distribution patterns, depending on the cooling rate applied to the sample. A Swiss cheese-like pattern in which many micrometer-sized dye-depleted regions are nucleated in a thin glycerol film can be observed upon slow cooling, whereas quick cooling gives rise to a spinodal decomposition pattern where micrometer-sized dye-enriched droplets are dispersed in a dye-depleted matrix.

Experimental Methods

Solutions of Alexa 488, Rhodamine 6G (R6G), and perylene-dicarboximide (PDI) in glycerol were prepared at 10^{-7} M. Alexa 594 and Alexa 488/polyproline 40 mer/Alexa 594 (dual-labeled) construct were prepared in glycerol at 10^{-8} and 10^{-9} M, respectively. The structures of the fluorophores and glycerol are shown in Figure 1. Anhydrous glycerol and PDI were purchased from Sigma-Aldrich Chemie BV (Netherlands). Alexa 488 and Alexa 594 were ordered from Invitrogen (Netherlands). R6G was purchased from Radiant Dye Laser (Germany). Dual-labeled proline 40 mer was synthesized in the Department of Biochemistry, University of Zurich. The glycerol solution was directly spin-coated at 6000 rpm on a round glass substrate with a diameter of 20 mm. To improve wetting, the glass substrates were first treated in a UV–ozone cleaner (model 42-220; Jelight,

* To whom correspondence should be addressed. Phone: (31) (0)71 527 1720/5910. Fax: (31) (0)71 527 5819. E-mail: orrit@molphys.leidenuniv.nl.

[†] Present address: College of Physics and Electronic Engineering, Shanxi University, Wu Cheng Lu 92, Taiyuan 030006, China.

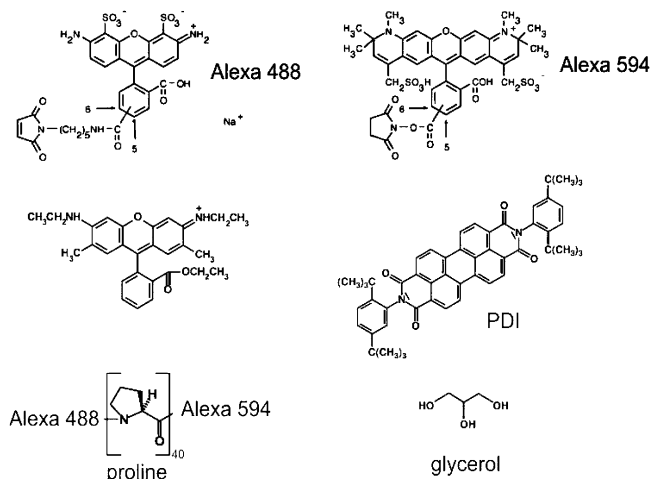


Figure 1. Structures of the fluorophores and glycerol.

Irvine, CA). The resulting thickness of the glycerol film from this procedure was $0.5\text{--}2\text{ }\mu\text{m}$, as deduced from examination in a home-built Michelson interferometer. To minimize water content in glycerol solution, the samples were dried in the cryostat by repeatedly pumping and flushing with helium gas at room temperature and kept under dry helium throughout all experiments.

The experiments were conducted with a home-built laser-scanning confocal microscope that allows for the optical experiments in the full temperature range from 1.5 K to room temperature. This setup is described in detail in ref 28. The slow cooling was done by cooling the sample from room temperature without precooling the cryostat, which leads to a nearly constant cooling rate of 5 K/h between 295 and 208 K. The quick cooling rate was achieved by quickly putting the sample from room temperature into the precooled cryostat whose temperature was 220 K. In this way, the sample experienced a very sudden temperature drop in the very beginning, and the cooling rate then decayed with time. Since the temperature went through the freezing point of water very fast, the drying procedure was not applied to the quickly cooled sample. Although the water content in this case is probably higher than that in the slowly cooled sample, we do not believe that the water traces change the properties of glycerol significantly (see Discussion section).

We excited the fluorescence at 488 nm with an argon ion laser (Spectra-Physics Stabilite 2017) and at 594 nm with a yellow HeNe laser (Melles Griot, 25LYP173-230). All of the images of $100 \times 100\text{ }\mu\text{m}^2$ were scanned with 200×200 pixels, a dwell time of 10 ms, and an excitation power of 2.0 kW/cm^2 for the fluorescence and 60 W/cm^2 for the scattering measurements.

Results

In this work, five different fluorescent probes (see Figure 1) were used to image thin glycerol films. All of the probes, except Alexa 488, showed a conspicuous long-lived heterogeneous pattern of the fluorescence intensity (Figure 2A–D) in glycerol at temperatures 15–18 K above T_g . This pattern is characterized by many micrometer-sized dark spots with a roughly circular shape, dispersed in a bright background, which resembles a cross section of a Swiss cheese with many holes. Although the shape and size of dark spots differ among and even within those samples, the bright and dark regions are quite distinguishable. Such cheese-like patterns become first detectable at temperatures

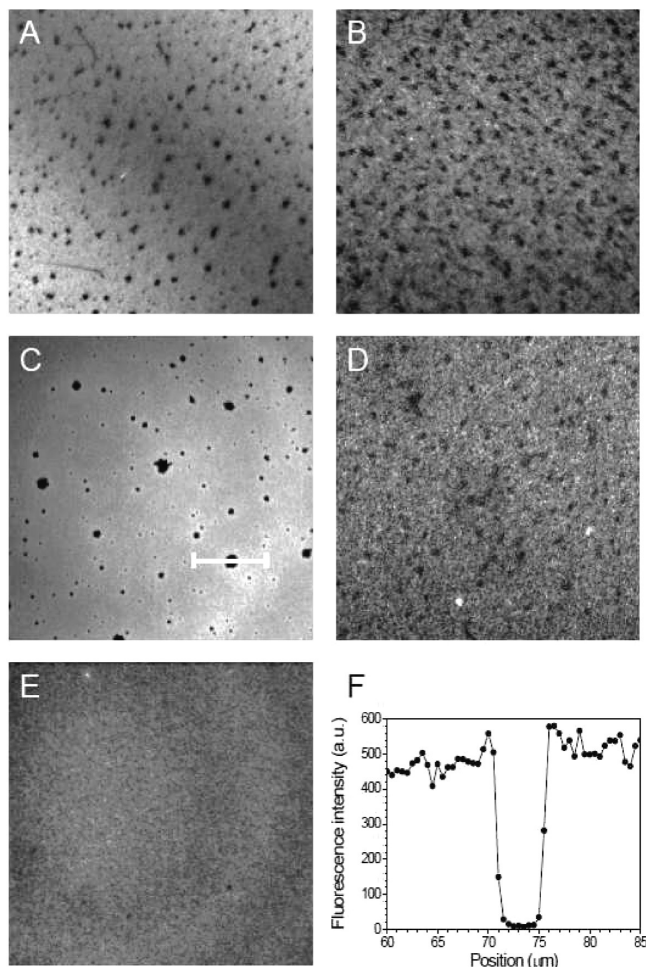


Figure 2. Confocal scanning images of different fluorescent probes in thin glycerol films at temperatures close to, but above, T_g . All of the images recorded are $100 \times 100\text{ }\mu\text{m}^2$. (A) Fluorescence image of Alexa 488/polyproline (40 mer)/Alexa 594 construct (10^{-9} M) excited by 594 nm laser at 206 K; (B) 10^{-7} M PDI excited by 488 nm laser at 208 K; (C) 10^{-7} M R6G in glycerol at 207 K; (D) 10^{-8} M Alexa 594 in glycerol at 205 K; (E) 10^{-7} M Alexa 488 in glycerol at 208 K. (F) One-dimensional fluorescence profile of a dark spot in C indicated by the white bar.

around 220 K (data not shown), which is 30 K above the glass transition temperature of glycerol. However, the cheese-like pattern was not clearly seen in the glycerol when doped with Alexa 488 (Figure 2E), where the fluorescence intensity was nearly homogeneous in the scanned field in the same temperature range. Once the cheese-like pattern is formed, it can persist for days unless the sample is heated up to 260 K and kept at this temperature for about 10 h. After this treatment, the pattern disappears and the fluorescence intensity becomes homogeneous (data not shown). If the heated sample is cooled down again toward glassy temperature, the cheese-like pattern will reappear reliably.

Figure 2F shows the one-dimensional fluorescence intensity profile of a dark spot of Figure 2C. The fluorescence intensity drops almost to the background level in the center of the dark region. If we assume that the probe molecules are homogeneously distributed in the sample, the fluorescence intensity would then be correlated to the thickness of the glycerol film. The observed dark spots should therefore stem from steep variations in the film thickness, resulting from the formation of physical holes, tentatively due to local dewetting. Another assumption would be that the thickness of the film is more or

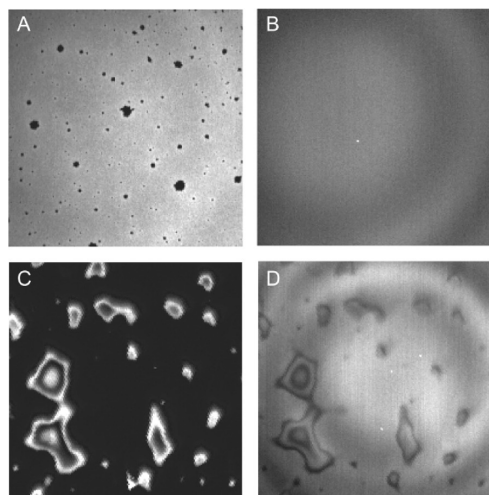


Figure 3. Comparison of fluorescence and scattering images ($100 \times 100 \mu\text{m}^2$). (A) Fluorescence image of 10^{-7} M R6G in glycerol reveals the cheese-like pattern at 207 K. (B) Scattering image of the same area in A does not show any of physical features, indicating that the thickness and index of refraction of the glycerol film are rather uniform in the scanned area. (C) Fluorescence image was taken from the sample (10^{-7} M PDI in glycerol) at 295 K, which was first heated up to 295 from 208 K and then kept at 295 K for 24 h. The image reveals many isolated bright features with irregular droplet and ring-like shapes, suggesting that the glycerol film is completely ruptured after a long time at room temperature due to dewetting. (D) Scattering image of the same region shows the same features as seen in C. Physical features can be detected by both fluorescence and scattering imaging. The concentric interference pattern seen in B and D is due to multiple reflection of the incident beam from the cryostat windows, which modulates the incident power during the beam scanning. This profile can be weakly seen in A as well.

less uniform within the scanned area and that either the local probe concentration or the fluorescence emissivity of the probe is not homogeneous on the length scale of a few micrometers. To test the first assumption, we imaged the sample directly with the laser light scattered from the surface. If there were any physical holes or morphological structure present in the sample, the incident light should be strongly scattered by the holes, resulting in a position-dependent signal in the scanned image. It should be noted that the scattering measurements here differ from conventional light scattering. In the latter method, an incident beam with a high power usually illuminates a sample with a thickness of some millimeters, and the intensity, angular dependence, or dynamical fluctuations of the scattered intensity provide information about refractive index fluctuations in the material. Here, we used a relatively weak laser beam to scan a thin film of glycerol (see Experimental Methods), so that only strong index fluctuations or morphological structures such as holes in the film would give rise to a measurable signal. Figure 3A again shows the fluorescence image of Rhodamine 6G (R6G) in glycerol (Figure 2C) revealing the cheese-like pattern. The right image was taken from the scattering measurement in the same area. The intensity of the scattered light is more or less homogeneous in the field of view (except for concentric interference fringes due to multiple reflections in the cryostat windows, which modulate the power of the incident light during the beam scanning). Since the scattering image does not show any sign of morphological features, the cheese-like pattern is not likely due to the formation of physical holes resulting from dewetting, but rather to a differential dye distribution or to a variable fluorescence brightness due to photophysics of the dyes (see Discussion section) in glycerol films. Control experiments shown in Figure 2C,D show that the rupture of the glycerol

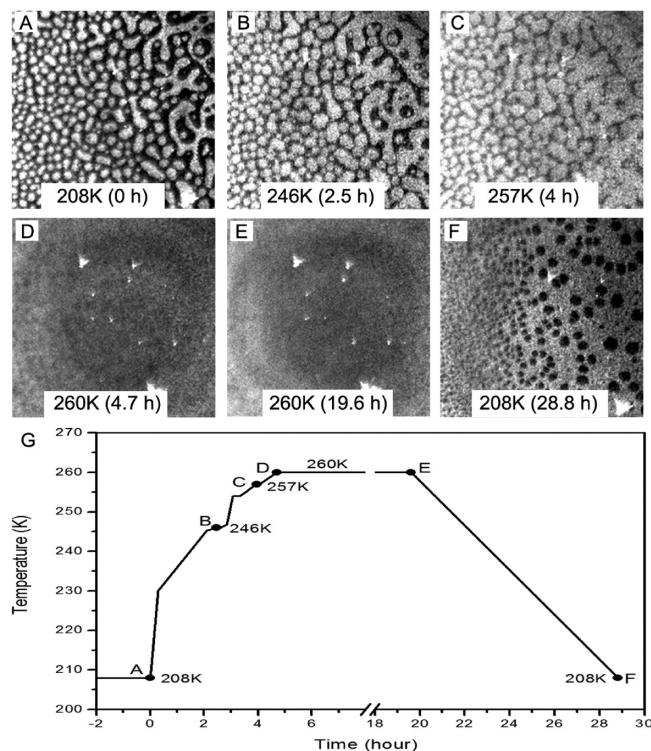


Figure 4. Sequential fluorescence images ($100 \times 100 \mu\text{m}^2$) of 10^{-7} M PDI in glycerol during first warming up (A–D) and then slow cooling down (E,F). The employed thermal history is shown in G, where the solid circles indicate the fluorescence measurements of A–F. Upon the initial quick cooling from room temperature, bright island-like features are separated by a dark matrix. The isolated bright features coarsen upon warming up, and neighboring features start to fuse into bigger ones. Finally, all bright features merge into one uniform bright region at 260 K, and the dark region disappears completely. After one night at 260 K, the sample was cooled slowly (5 K/h) down to 208 K and the cheese-like pattern appeared.

film resulting from dewetting at room temperature can be reliably detected by both fluorescence and scattering imaging.

A previous rheological study on glycerol indicates that the behavior of supercooled glycerol is strongly dependent on the thermal history;²⁰ in particular, the cooling rate is one of the important factors. The above-mentioned cheese-like pattern was observed from the samples that had an average cooling rate of 5 K/h starting from room temperature. If the sample was cooled down to 208 K with a quick cooling rate (see Experimental Methods), it showed a quite different pattern (see Figure 4A). Instead of a cheese-like pattern in which many dark spots are nucleated in the bright matrix, bright micrometer-sized and island-like features are formed in a dark matrix, which resembles a spinodal decomposition pattern. The bright features in the left part of the image are more circular in shape and smaller, whereas features in the right part of the image are more branched, elongated, and bigger. Such a gradient across the sample may originate from a slight variation of the film thickness from the right (thin) to the left (thick). Because the cheese-like pattern disappeared upon heating the slowly cooled sample at 260 K for more than 10 h, the same thermal treatment was also applied to the fast cooled sample. Figure 4A–F shows sequential fluorescence images of PDI in glycerol as a function of temperature and the thermal history of the sample is indicated in (G). Upon heating up from 208 K, the isolated bright features first coarsened, then neighboring small features started to contact one another and fused to bigger ones. Meanwhile, the dark area kept shrinking along with this heating process. Finally, all of

the big bright features merged into one uniform bright area at 260 K, and the dark area vanished completely. This evolution of the fluorescence pattern mainly takes place at higher temperatures. Annealing the sample at a fixed temperature well below 260 K does not give any significant change of the pattern on the time scale of hours (data not shown). The bright island-like features observed at 208 K disappeared upon heating the sample to 260 K. However, the cheese-like pattern formed again from the same sample upon slow cooling down (5 K/h) to 208 K. Clearly, the cooling rate influences the pattern of the fluorescence intensity in supercooled glycerol.

Discussion

We have chosen five fluorescent probes to image supercooled glycerol, and the cheese-like pattern was observed with dual-labeled polypyrrolone 40 mer, PDI, Alexa 594 and R6G, but not with Alexa 488. The dark areas in the cheese-like patterns revealed by those different probes are quite different in terms of size, shape, and density. We tentatively attribute those differences to the different experimental conditions (e.g., the thickness of the films, the concentration of the dyes, and the chemical nature of the probes). Scattering measurements on the cheese-like pattern indicate no obvious morphological features in the glycerol film, which leaves two other possible origins responsible for the heterogeneous pattern of the fluorescence intensity. (i) The dye distribution is heterogeneous. (ii) The dye distribution is homogeneous, but its fluorescence brightness is not uniform in the sample due to its photophysics (e.g., the photophysics of a long-lived dark state). Early work shows that R6G can form a radical ion from the triplet state in polyvinyl alcohol, which leads to a long-lived dark state.²⁷ Similar photophysics were seen in R6G/glycerol, where the lifetime of this dark state has a strong temperature dependence between 280 and 200 K.²⁸ However, PDI is rather photostable, and its fluorescence emissivity is almost independent of temperature.¹⁶ If the photophysics of R6G are the cause of the cheese-like pattern in R6G/glycerol sample, then PDI should give a much lower contrast. Both R6G and PDI showed the cheese-like pattern, suggesting that such a pattern is unlikely to be due to photophysics of the dyes. Therefore, we assume that a non-uniform dye distribution in the sample is responsible for the observed cheese-like pattern.

One obvious question is whether the observed cheese-like pattern is probe-induced or an intrinsic property of supercooled glycerol that can be sensed by the probes. The following arguments can rule out the probe-induced hypothesis: First, the concentrations of all five probes used in this work are rather low, ranging from 10^{-7} to 10^{-9} M. Such low concentrations of probes are not expected to influence the properties of glycerol significantly. Second, dual-labeled polypyrrolone 40 mer, PDI, Alexa 594, and R6G differ in many aspects, such as size, structure, and chemical properties (Figure 1), but they all show similar dye distribution patterns. Therefore, the observed cheese-like pattern is probably not induced by the probes, but rather an intrinsic property of supercooled glycerol made visible by the probes.

Light and X-ray scattering experiments have indicated that density fluctuations occur in supercooled liquids when they are cooled toward their glass transition temperatures.^{10,11,29} When supercooled glycerol is cooled close to T_g , the system may start to develop (or nucleate) regions that have higher density than their surroundings. It is then natural to assume that the observed heterogeneous pattern of the fluorescence intensity at temperatures close to T_g is related to density fluctuations in the glycerol

film. Since the system begins in the pure liquid state in which the fluorescence is homogeneous over the sample, it is very likely that bright areas have a close-to-normal density and the dark areas a higher density. The local glycerol structures in such denser and darker regions may be less disordered or more solid-like. When the probes are added into the glycerol, they may be less easily incorporated into such local ordered structures and therefore are segregated out of these regions. Segregation results from a lower solubility of probes in solid-like parts than in liquid-like regions with the normal liquid density, provided that translational diffusion of the probes is fast enough during the cooling process. Similar segregation is also seen in membrane^{24,25} and other 2D systems.³⁰ According to this interpretation, the size of dark areas in the fluorescence image corresponds to the size of solid-like domains. We propose that the relatively strong polarity of Alexa 488 is the reason why it did not show the cheese-like pattern in glycerol because it would interact more strongly with glycerol through hydrogen bonds.

Since the coexistence of liquid and solid-like structures in supercooled glycerol above T_g has been confirmed by rheological experiments,¹⁶ it is not very surprising to see two distinct dark (solid-like) and bright (liquid) regions in the same temperature range. However, a further growth of the solid-like network in glycerol, which was seen in the rheology, was not observed from the fluorescence images at temperatures between 220 and 190 K. Namely, the size of dark spots remains fairly constant in this temperature range. Experimental conditions (e.g., sample volumes, thickness of films, and contact surfaces) in these two experiments are quite different. In the rheological experiments, the glycerol resided in a 2 mm gap of a Couette cell, which was made of brass and held about 9 mL of sample. Here, a glycerol film with a thickness of a few micrometers was coated on a glass substrate with a diameter of 20 mm. Therefore, the behaviors of glycerol in these two experiments could be different as well. The picture we have in mind is the following. The solid-like structures appear already at temperatures above 220 K. Since the fluorescence is homogeneous at 260 K, the nucleation and growth of solid-like structures perhaps take place between 260 and 220 K, where the viscosities of glycerol are not large enough to prevent the probes from being pushed away from the growing solid-like structures. However, between 220 and 190 K, this redistribution of the probes due to the growth of the solid-like structures is slowed down and even arrested because of the extremely large viscosities in this temperature range. Therefore, the size of the dark spots remains nearly the same even at temperatures below T_g (data not shown).

Another interesting finding is that the fluorescence patterns resulting from slow and quick cooling are quite distinct. In the slowly cooled samples, nucleated micrometer-sized dark spots are dispersed in a bright background. In the quickly cooled sample, however, bright micrometer-sized features are isolated by a dark matrix. Such phenomena are very analogous to nucleation and spinodal decomposition behaviors of phase separation in a two-component system, respectively.³¹ Triphenyl phosphite (TPP), another molecular glass-former, was also found to show solid-like behavior at temperatures above its glass transition.^{32–35} This apparently amorphous phase was denoted as the glacial phase, a new amorphous phase distinct from both the glass and crystal.^{34,35} Moreover, two types of phase transformation have been seen in TPP as well, depending on the annealing temperature. The nucleation–growth type of phase transformation was observed at a higher annealing temperature ($T_g + 15$ K), and the spinodal decomposition type of transformation happened at a lower temperature ($T_g + 8$ K).^{32,33} These

observations from TPP are very similar to what we found here for glycerol. However, these two molecular liquids also show several dissimilarities. First, both types of phase transformation in TPP are more or less complete and lead to the glacial phase.^{34,35} In contrast, the cheese-like and spinodal decomposition patterns are rather stable in glycerol at a fixed temperature below 260 K. Second, whereas in TPP the temperature alone determines the phase, in glycerol, the cooling rate plays an equally important part. Lastly, the heterogeneous fluorescence patterns in glycerol from both quick and slow cooling became homogeneous again upon heating at 260 K for more than 10 h, which suggests that the solid-like structures formed at low temperature in both cases are free from large microcrystallites since the growth of a crystal is more favored at higher temperature once large enough seeds are formed. In the case of TPP, the glacial phase resulting from spinodal decomposition is free from microcrystallites, whereas the final state of nucleation–growth transformation is a mixture of the new amorphous phase and microcrystallites.³¹ When heated up above 240 K, TPP from both types of transformation turns into a crystal.

More interestingly, the cheese-like pattern in glycerol can be observed in a previously quickly quenched sample upon heating to 260 K and slow cooling again, indicating that keeping the sample at 260 K for a long period can effectively melt the dense or solid-like structures. This observation not only confirms that the glycerol remained liquid-like at 260 K but also excludes the possibility that water traces are responsible for the observed heterogeneous patterns since the fluorescence intensity became homogeneous at 260 K (see Figure 4E), 12 K below the freezing point of water. Additionally, the cheese-like pattern appeared again upon slow cooling of the quickly quenched sample (see Figure 4F). This additional “melting point” suggests the existence of a “liquid–liquid phase transition” or LLP in a single-component liquid,^{32,33,36} although the observations here are not the same. Whether the observed solid-like structure in glycerol is related to the glacial phase of TPP or to Fischer clusters is not yet clear. The length scale of heterogeneity in supercooled glycerol revealed by fluorescence imaging is on the order of micrometers, bridging the gap between the millimeter scale of rheological measurements¹⁶ and the nanometer scale of single-molecule fluorescence.²⁰

Conclusion

We observed a heterogeneous fluorescence pattern in supercooled glycerol doped with fluorescent probes. Such a heterogeneous pattern resulting from a differential dye distribution reveals micrometer-sized structures with an extremely long lifetime and appears to be connected to the long-lived density fluctuations on micrometer scale in supercooled glycerol postulated earlier.¹⁶ Moreover, the structure of the heterogeneous pattern is clearly influenced by the cooling rate. A slow cooling leads to a cheese-like pattern, whereas a quick cooling results in a spinodal decomposition pattern. More work is needed to characterize such heterogeneous patterns, for example, a study of the mobility of probes in the dark and bright regions will give more local structural information, which may help better to understand the complex behavior of supercooled molecular liquids.

Acknowledgment. We thank Prof. Benjamin Schuler for kindly providing us with dual-labeled polyproline samples. This work is part of the research program of the “Stichting voor

Fundamenteel Onderzoek der Materie” (FOM), which is financially supported by The Netherlands Organization for Scientific Research.

References and Notes

- (1) de Gennes, P. G. A simple picture for structural glasses. *C.R. Phys.* **2002**, *3*, 1263–1268.
- (2) Sillescu, H. Heterogeneity at the glass transition: A review. *J. Non-Cryst. Solids* **1999**, *243*, 81–108.
- (3) Hurley, M. M.; Harrowell, P. Kinetic structure of a 2-dimensional liquid. *Phys. Rev. E* **1995**, *52*, 1694–1698.
- (4) Bennemann, C.; Donati, C.; Baschnagel, J.; Glotzer, S. C. Growing range of correlated motion in a polymer melt on cooling towards the glass transition. *Nature* **1999**, *399*, 246–249.
- (5) Stevenson, J. D.; Schmalian, J.; Wolynes, P. G. The shapes of cooperatively rearranging regions in glass-forming liquids. *Nat. Phys.* **2006**, *2*, 268–274.
- (6) Diezemann, G.; Böhmer, R.; Hinze, G.; Sillescu, H. Reorientational dynamics in simple supercooled liquids. *J. Non-Cryst. Solids* **1998**, *235*, 121–127.
- (7) Tracht, U.; Wilhelm, M.; Heuer, A.; Feng, H.; Schmidt-Rohr, K.; Spiess, H. W. Length scale of dynamic heterogeneities at the glass transition determined by multidimensional nuclear magnetic resonance. *Phys. Rev. Lett.* **1998**, *81*, 2727–2730.
- (8) Schiener, B.; Chamberlin, R. V.; Diezemann, G.; Böhmer, R. Nonresonant dielectric hole burning spectroscopy of supercooled liquids. *J. Chem. Phys.* **1997**, *107*, 7746–7761.
- (9) Schneider, U.; Lunkenheimer, P.; Brand, R.; Loidl, A. Dielectric and far-infrared spectroscopy of glycerol. *J. Non-Cryst. Solids* **1998**, *235*, 173–179.
- (10) Patkowski, A.; Thurn-Albrecht, Th.; Banachowicz, E.; Steffen, W.; Bösecke, P.; Narayanan, T.; Fischer, E. W. Long-range density fluctuations in orthoterphenyl as studied by means of ultrasmall-angle X-ray scattering. *Phys. Rev. E* **2000**, *61*, 6909–6913.
- (11) Patkowski, A.; Fischer, E. W.; Steffen, W.; Gläser, H.; Baumann, M.; Ruths, T.; Meier, G. Unusual features of long-range density fluctuations in glass-forming organic liquids: A Rayleigh and Rayleigh–Brillouin light scattering study. *Phys. Rev. E* **2001**, *63*, 061503.
- (12) Cicerone, M. T.; Ediger, M. D. Enhanced translation of probe molecules in supercooled *o*-terphenyl: Signature of spatially heterogeneous dynamics. *J. Chem. Phys.* **1996**, *104*, 7210–7218.
- (13) Ediger, M. D. Spatially heterogeneous dynamics in supercooled liquids. *Annu. Rev. Phys. Chem.* **2000**, *51*, 99–128.
- (14) Deschenes, L. A.; Vanden Bout, D. A. Heterogeneous dynamics and domains in supercooled *o*-terphenyl: A single molecule study. *J. Phys. Chem. B* **2002**, *106*, 11438–11445.
- (15) Schob, A.; Cichos, F.; Schuster, J.; von Borczyskowski, C. Reorientation and translation of individual dye molecules in a polymer matrix. *Eur. Polym. J.* **2004**, *40*, 1019–1026.
- (16) Zondervan, R.; Kulzer, F.; Berkhout, G. C. G.; Orrit, M. Local viscosity of supercooled glycerol near T_g probed by rotational diffusion of ensembles and single dye molecules. *Proc. Natl. Acad. Sci. U.S.A.* **2007**, *104*, 12628–12633.
- (17) Miller, R. S.; MacPhail, R. A. Ultraslow nonequilibrium dynamics in supercooled glycerol by stimulated Brillouin gain spectroscopy. *J. Chem. Phys.* **1997**, *106*, 3393–3401.
- (18) Miller, R. S.; MacPhail, R. A. Physical aging in supercooled glycerol: Evidence for heterogeneous dynamics. *J. Phys. Chem. B* **1997**, *101*, 8635–8641.
- (19) Reinsberg, S. A.; Qiu, X. H.; Wilhelm, M.; Spiess, H. W.; Ediger, M. D. Length scale of dynamic heterogeneity in supercooled glycerol near T_g . *J. Chem. Phys.* **2001**, *114*, 7299–7302.
- (20) Zondervan, R.; Xia, T.; van der Meer, H.; Storm, C.; Kulzer, F.; van Saarloos, W.; Orrit, M. Soft glassy rheology of supercooled molecular liquids. *Proc. Natl. Acad. Sci. U.S.A.* **2008**, *105*, 4493–4498.
- (21) Jinnai, H.; Yoshida, H.; Kimishima, K.; Funaki, Y.; Hirokawa, Y.; Ribbe, A. E.; Hashimoto, H. Observation of fine structures in bicontinuous phase-separated domains of a polymer blend by laser scanning confocal microscopy. *Macromolecules* **2001**, *34*, 5186–5191.
- (22) Aoki, H.; Sakurai, Y.; Ito, S.; Nakagawa, T. Phase-separation structure of a monolayer of binary polymer blend studied by fluorescence scanning near-field optical microscopy. *J. Phys. Chem. B* **1999**, *103*, 10553–10556.
- (23) Hirokawa, Y.; Jinnai, H.; Nishikawa, Y.; Okamoto, T.; Hashimoto, T. Direct observation of internal structures in poly(*N*-isopropylacrylamide) chemical gels. *Macromolecules* **1999**, *32*, 7093–7099.
- (24) Helm, C. A.; Möhwald, H.; Kjaer, K.; Als-Nielsen, J. Phospholipid monolayers between fluid and solid states. *Biophys. J.* **1987**, *52*, 381–390.
- (25) Baumgart, T.; Hess, S. T.; Webb, W. W. Imaging coexisting fluid domains in biomembrane models coupling curvature and line tension. *Nature* **2003**, *425*, 821–824.

- (26) Veatch, S. L.; Keller, S. Separation of liquid phases in giant vesicles of ternary mixtures of phospholipids and cholesterol. *Biophys. J.* **2003**, *85*, 3074–3083.
- (27) Zondervan, R.; Kulzer, F.; Orlinskii, S. B.; Orrit, M. Photoblinking of rhodamine 6G in poly(vinyl alcohol): Radical dark state formed through the triplet. *J. Phys. Chem. A* **2003**, *107*, 6770–6776.
- (28) Zondervan, R.; Kulzer, F.; van der Meer, H.; Disselhorst, J. A. J. M.; Orrit, M. Laser-driven microsecond temperature cycles analyzed by fluorescence polarization microscopy. *Biophys. J.* **2006**, *90*, 2958–2969.
- (29) Fischer, E. W. Light-scattering and dielectric studies on glass-forming liquids. *Physica A* **1993**, *201*, 183–206.
- (30) Kurita, R.; Murata, K.; Tanaka, H. Control of fluidity and miscibility of a binary liquid mixture by the liquid–liquid transition. *Nat. Mater.* **2008**, *7*, 647–652.
- (31) Donald, A. Food for thought. *Nat. Mater.* **2004**, *3*, 579–581.
- (32) Tanaka, H.; Kurita, R.; Mataki, H. Liquid–liquid transition in the molecular liquid triphenyl phosphite. *Phys. Rev. Lett.* **2004**, *92*, 025701–025704.
- (33) Kurita, R.; Tanaka, H. Critical-like phenomena associated with liquid–liquid transition in a molecular liquid. *Science* **2004**, *306*, 845–848.
- (34) Cohen, I.; Ha, A.; Zhao, X. L.; Lee, M.; Fischer, T.; Strouse, M. J.; Kivelson, D. A low-temperature amorphous phase in a fragile glass-forming substance. *J. Phys. Chem.* **1996**, *100*, 8518–8526.
- (35) Ha, A.; Cohen, I.; Zhao, X. L.; Lee, M.; Kivelson, D. Supercooled liquids and polyamorphism. *J. Phys. Chem.* **1996**, *100*, 1–4.
- (36) Tanaka, H. General view of a liquid–liquid phase transition. *Phys. Rev. E* **2000**, *62*, 6968–6976.

JP9058388